Chinese Science Bulletin

Geochronologic and petrochemical evidence for the genetic link between the Maomaogou nepheline syenites and the Emeishan large igneous province

LUO ZhenYu[1,2†], XU YiGang[1], HE Bin[1], SHI YuRuo[3] & HUANG XiaoLong[1]

1. Key Laboratory of Isotope Geochronology and Geochemistry, Guangzhou Institute of Geochemistry, Chinese Academy of Sciences, Guangzhou 510640, China;
2. Graduate University of the Chinese Academy of Sciences, Beijing 100049, China;
3. Beijing SHRIMP Center, Beijing 100037, China

The Maomaogou nepheline syenite is located at the inner zone of the Emeishan large igneous province and exhibits intrusive contact with the Emeishan basalts. SHRIMP U-Pb dating on zircons from this syenite yields an age of 261.6±4.4 Ma, in agreement with the age of the Panzhihua layered intrusion and the eruption age of the Emeishan basalts as constrained by stratigraphic data. Geochemical data further suggest that the Maomaogou syenite has a source analogue to the Emeishan basalt, and may have been formed by partial melting of gabbroic cumulates underplated in the lower crust. As s result, temporal and spatial relationships and petrogenetic constraints provide evidence for the genetic link between basalts, mafic/ultramafic and intermediate/acidic intrusives in the Panxi area.

nepheline syenite, SHRIMP U-Pb dating, petrogenesis, Maomaogou, Emeishan LIP

The Late Permian Emeishan flood basalts and associated rocks, widely distributed in Sichuan, Guizhou and Yunnan provinces, are the only pertinent large igneous province (LIP) in China, which is recognized by international community[1−3]. Because many lines of evidence suggest that the Emeishan flood volcanism was responsible for the end-Guadalupian mass extinction[2,3], it is therefore pivotal to determine the age and duration of the Emeishan volcanism. However, the general absence of zircons in mafic extrusive rocks and severe later thermal perturbation of Ar-Ar isotopic system[4,5] render the direct dating of the Emeishan basalts difficult. A suite of mafic/ultramafic and intermediate/acidic intrusives, closely associated with the Emeishan basalts, is exposed in the Panzhihua-Xichang area (abbreviated as "Panxi area"). It has been argued that these three different types of rocks are genetically related to each other (Chinese geologists termed this a "Trinity" character[6]). If this is correct, dating intermediate/acidic intrusive rocks would be a clue to constrain the eruptive age of the Emeishan volcanism. In addition, geochemical analyses could provide insight into the origin of intrusive rocks in this LIP.

The Maomaogou nepheline syenites are typical of alkaline intrusive rocks in the Panxi area. Recent chronological studies suggest that this intrusion was emplaced at 216−253 Ma[7,8]. These ages are significantly different from the age of Emeishan basalts (258−260 Ma) constrained by stratigraphic data[9], casting doubt on the "Trinity" argument. Given the importance of the Maomaogou intrusion in the study of the Emeishan LIP and the failure of application of Ar-Ar method to Emeishan basalts, we re-visited this intrusion and carried out petrology, geochemical and SHRIMP zircon U-Pb analyses.

Received May 9, 2006; accepted August 28, 2006
doi: 10.1007/s11434-007-0112-5
†Corresponding author (email: zhenyuluo@gig.ac.cn)
Supported by the National Natural Science Foundation of China (Grant Nos. 40421303 and 40234046)

Both petrogenetic evaluation and geochronological data lead to the conclusion that these intermediate/acidic intrusives are genetically and temporally linked to the Emeishan basalts.

1 Geological background and samples

The Panxi area, also called Panxi paleo-rift, is located in the western margin of the Yangtze Block and in the inner zone of the Emeishan LIP (Figure 1(a)). There are abundant magmatism and mineral resources in this area. The basement is Middle Proterozoic gneiss. Several large layered intrusions occur along the Panxi rift, including Taihe, Xinjie, Hongge and Panzhihua intrusions. These intrusions, being predominantly of mafic/ultramafic composition with subordinate intermediate/acidic alkaline intrusive rocks, intrude the Emeishan basalts and Precambian Dengying marbles. While the Emeishan basalts and mafic/ultramafic intrusions are considered as the product of the Emeishan plume activity, little is known as to the age and petrogenesis of intermediate/acidic alkaline intrusions.

The Maomaogou intrusion is located in the Huili County, Sichuan Province, to the NNE of Longzhou Mountain, and at the middle part of the inner zone of the Emeishan LIP (Inner zone was defined by He et al.[10]). This intrusion is distributed along the N-S trending Anninghe-Yimen fault. It is ~15 km in length and ~2.3 km in width covering an area of ~32 km^2. The intrusion is circular in shape with diorite in core and nepheline syenites as envelop. It intrudes the late Permian Emeishan basalts (Figure 1(c)), Early Permian limestones and Ordovician sandstones, and is in turn cut by dioritic dykes. Nepheline syenite, which is the object of this study, has a coarse granular texture with feldspar reaching 10 mm in length. It mainly consists of microcline, albite, nepheline, hedenbergite, ferropargasite, sodalite, Ti-magnetite and minor biotite.

2 Analytical methods and results

2.1 Zircon U-Pb dating and Hf isotopes

Zircons were separated using conventional heavy liquid and magnetic techniques. Grains were handpicked under binocular microscope and mounted in an epoxy resin disc, and then polished. Internal structure was examined

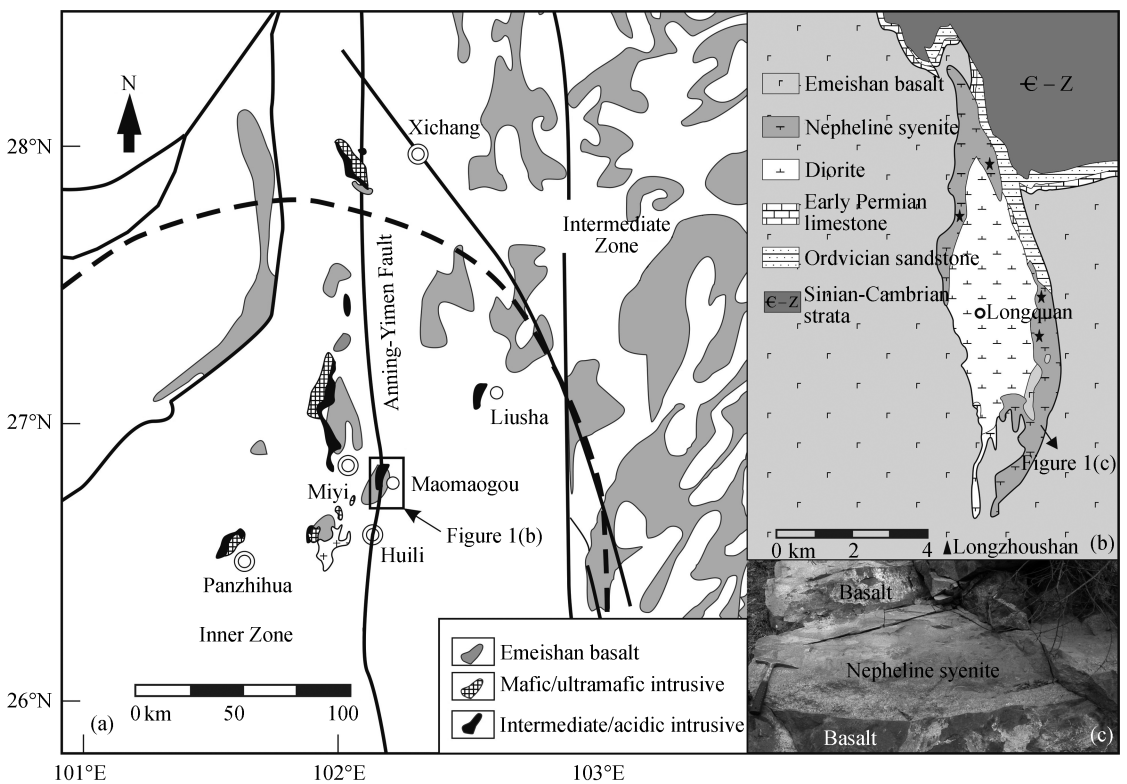

Figure 1 (a) Schematic geological map in the Panxi area; (b) map showing the details of the Maomaogou intrusions; (c) photo showing intrusion of the Maomaogou nepheline syenite in the Emeishan basalt. Solid pentagrams in (b) represent sample sites.

using cathodoluminescence (CL) images prior to U-Pb isotopic analyses. The U-Pb analyses were performed using the Sensitive High-Resolution Ion Microprobe (SHRIMP II) at the Chinese Academy of Geological Sciences in Beijing. Detailed analytical procedures are similar to those described by Compston et al. and Williams[11,12]. The interelement fractionation was corrected by using RSES referenced zircon TEM (417 Ma), and U, Th and Pb concentrations were determined relative to that of the standard Sri Lankan gem zircon SL13, which has a U concentration of 238 ppm corresponding to an age of 572 Ma. Data processing procedures are after LudwigSQUID1.0 and ISOPLOT programs. Common Pb was corrected by using observed ^{204}Pb. Uncertainties listed in Table 1 are given at ±1σ. The ages quoted in the text are ^{206}Pb/^{238}U ages, which are the weighted mean at the 95% confidence level.

CL images are important and effective to distinguish magmatic zircons from metamorphic zircons. Zircons of magmatic origin are generally characterized by oscillatory zoning, whereas metamorphic zircons are characterized by radial sector overgrowth zoning, planar overgrowth banding or the patches without zoning[13−15]. The zircons extracted from the Maomaogou nepheline syenites are colorless, transparent and some of them clearly have micro-scale oscillatory zonings. None of them has core-rim structure. All these imply a primitive magmatic origin (Figure 2(b)). Th and U concentrations of magmatic zircon are generally high, and its Th/U ratio is commonly higher than 0.4, whereas those contents of metamorphic zircon are relatively low with its Th/U ratio < 0.1[16,17]. Analyses on 14 zircon grains from LQ-3 show relatively high Th and U contents and have Th/U ratios ranging between 0.39 and 1.04 (Table 1), reflect

Table 1 SHRIMP U-Pb isotopic data of zircons from the Maomaogou nepheline syenite (LQ-3)

Grain spot	U (ppm)	Th (ppm)	Th/U	^{206}Pb (ppm)	f_{206} a) (%)	^{207}Pb/^{206}Pb (±1σ)	^{207}Pb/^{235}U (±1σ)	^{206}Pb/^{238}U (±1σ)	Age (Ma) ^{206}Pb/^{238}U	Age (Ma) ^{207}Pb/^{206}Pb
1	180	155	0.86	6.49	0.92	0.0521±4	0.298±5	0.0415±3	262.1±6.8	290±93
2	215	180	0.84	8.01	0.80	0.0570±5	0.338±6	0.0430±3	271.1±6.8	492±110
3	149	104	0.70	5.38	2.70	0.0467±14	0.264±14	0.0409±3	258.3±7.1	36±330
4	476	427	0.90	17.4	0.91	0.0493±6	0.286±6	0.0421±2	265.7±6.3	162±130
5	181	71	0.39	6.41	2.41	0.0408±14	0.226±14	0.0403±3	254.5±7.0	–302±360
6	134	66	0.49	4.86	2.90	0.0498±19	0.281±19	0.0409±3	258.5±7.9	186±440
7	142	99	0.69	5.28	1.53	0.0527±13	0.310±13	0.0427±3	269.4±7.3	315±290
8	142	99	0.70	4.77	1.44	0.0539±11	0.287±11	0.0387±3	244.5±6.7	366±250
9	285	127	0.44	10.6	1.59	0.0453±12	0.267±12	0.0427±3	269.5±6.8	–38±280
10	101	51	0.50	3.93	2.61	0.0489±18	0.298±19	0.0442±7	279.0±18	144±420
11	421	213	0.51	14.4	0.38	0.0529±4	0.289±5	0.0396±3	250.3±7.2	324±89
12	381	395	1.04	13.3	0.43	0.0526±4	0.293±4	0.0404±2	255.6±6.2	311±84
13	908	354	0.39	18.5	0.58	0.0512±4	0.167±9	0.0236±8	150.0±12	250±98
14	241	99	0.41	9.41	1.23	0.0617±11	0.381±12	0.0449±6	283.0±17	663±230

a) f_{206}(%) is percentage of total ^{206}Pb which is non-radiogenic.

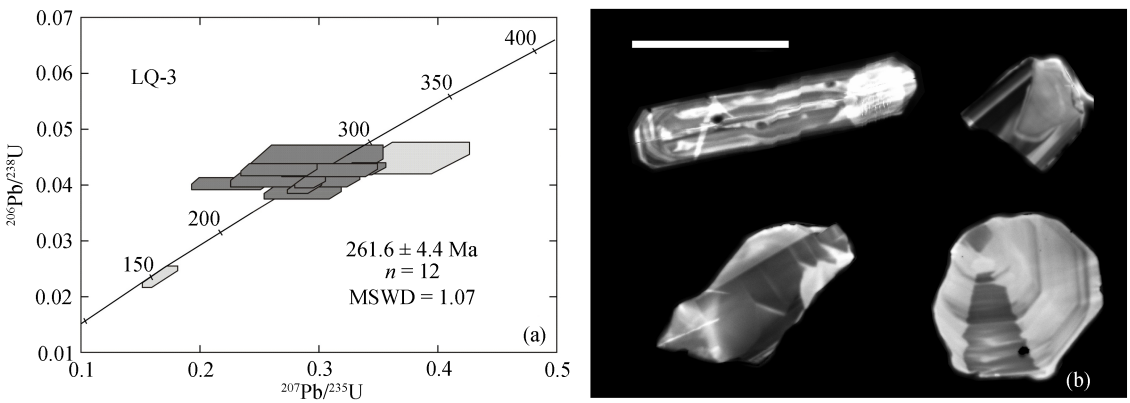

Figure 2 (a) U-Pb zircon concordia diagram for the Maomaogou nepheline syenite; (b) selected CL images of typical zircons. The bar in (b) is 100 μm.

ing their magmatic origin.

Twelve out of 14 analyses (Table 1) yield concordant $^{206}Pb/^{238}U$ ages (245－279 Ma). A weighted mean $^{206}Pb/^{238}U$ age of 261.6±4.4 Ma is obtained (Figure 2(a)). This age is interpreted as the timing of emplacement of the Maomaogou nepheline syenite.

Zircon Hf isotopic analysis was conducted on the Neptune MC-ICPMS equipped with a 193 nm laser at the Institute of Geology and Geophysics, Chinese Academy of Sciences, Beijing. The spot sizes were 31.5 or 63 μm with an ablation time of about 26 s. Zircon 91500 was used as a standard. The velocity of laser impulse is 8－10 Hz and the energy is 100 mJ. Detailed analytical procedure was described by Xu et al.[18]. The weighted average $^{176}Hf/^{177}Hf$ ratio of zircon 91500 during analyses is 0.282282±29, in agreement within errors with those obtained by the solution method[19,20].

Hf isotopic data of zircons are listed in Table 2. $^{176}Lu/^{177}Hf$ ratios of all zircons are less than 0.003 with an average ratio of 0.001, indicating a low radiogenetic growth of ^{176}Hf. While the spot 13 yields a relatively low $^{176}Hf/^{177}Hf$ ratio, all the other spots have $^{176}Hf/^{177}Hf$ ratios of 0.28257 to 0.28274 with $\varepsilon_{Hf}(t$ = 260 Ma) between –1.4 and +4.3.

2.2 Major and trace element compositions and Nd isotopes

Analyses of major, trace element composition and Nd isotopes were carried out in the Key Laboratory of Isotopic Chronology and Geochemistry, Guangzhou Institute of Geochemistry, Chinese Academy of Sciences, using XRF, ICP-MS and Micromass MC-ICPMS, respectively. The results are listed in Table 3.

The Maomaogou samples are intermediate in SiO_2 (53.99 %－55.79%), alkali-rich (Na_2O+K_2O =11.1%－13.0%) and low in K_2O/Na_2O (0.27－0.32). These samples are plotted in "nepheline syenite" field in TAS classification diagram. They exhibit high concentrations of Ba (505－1051ppm), Ga (22－23 ppm), Zr (110－191ppm), weak depletion in Ti, but with no Nb and Ta anomalies. In Figure 3(a), data of Liu et al.[8] are also plotted for comparison. It is shown that two datasets are basically in good agreement (Figure 3(a), (b)), suggesting that two independent studies were carried on the same rocks. The initial $^{143}Nd/^{144}Nd$ ratio (calculated at 260 Ma) is list in Table 3. $\varepsilon_{Nd}(t)$ varies between –0.73 and +1.44.

Table 2 Hf isotopic data of zircons from the Maomaogou nepheline syenite (LQ-3)[a)]

Grain spot	Type	Corresponding U-Pb spot	$^{176}Yb/^{177}Hf$	$^{176}Lu/^{177}Hf$	$^{176}Hf/^{177}Hf$	2σ	$\varepsilon_{Hf}(t)$	T_{DM} (Ga)
1	m	1	0.064172	0.002072	0.282735	0.000032	4.1	0.753
2	c	2	0.078585	0.002350	0.282736	0.000035	4.1	0.758
3	w	3	0.045770	0.001496	0.282717	0.000029	3.5	0.769
4	w	4	0.031456	0.001033	0.282640	0.000030	0.9	0.868
5	m	5	0.012783	0.000401	0.282630	0.000031	0.7	0.866
6	r	6	0.018320	0.000499	0.282600	0.000033	–0.4	0.910
7	r	7	0.037061	0.001174	0.282694	0.000030	2.8	0.794
8	c	8	0.037681	0.001122	0.282626	0.000036	0.4	0.889
9	m	9	0.023410	0.000656	0.282678	0.000029	2.3	0.805
10	w	10	0.018288	0.000599	0.282640	0.000032	1.0	0.857
11	w	11	0.013569	0.000526	0.282574	0.000026	–1.4	0.948
12	r	none	0.014178	0.000507	0.282653	0.000048	1.5	0.837
13	w	13	0.035542	0.001388	0.282407	0.000039	–9.8	1.207
14	r	14	0.018045	0.000695	0.282624	0.000026	0.4	0.881
15	m	none	0.014747	0.000564	0.282636	0.000043	0.8	0.862
16	m	12	0.072572	0.002821	0.282613	0.000034	–0.4	0.951
17	m	none	0.015566	0.000504	0.282691	0.000046	2.8	0.784
18	c	none	0.022525	0.000796	0.282650	0.000030	1.3	0.848
19	c	none	0.066437	0.002075	0.282740	0.000030	4.3	0.746
20	m	none	0.021506	0.000716	0.282581	0.000040	–1.1	0.943

a) $\varepsilon_{Hf}(t)$ was calculated to be 260 Ma. r, rim; m, mantle; c, core; w, whole zircon grain.

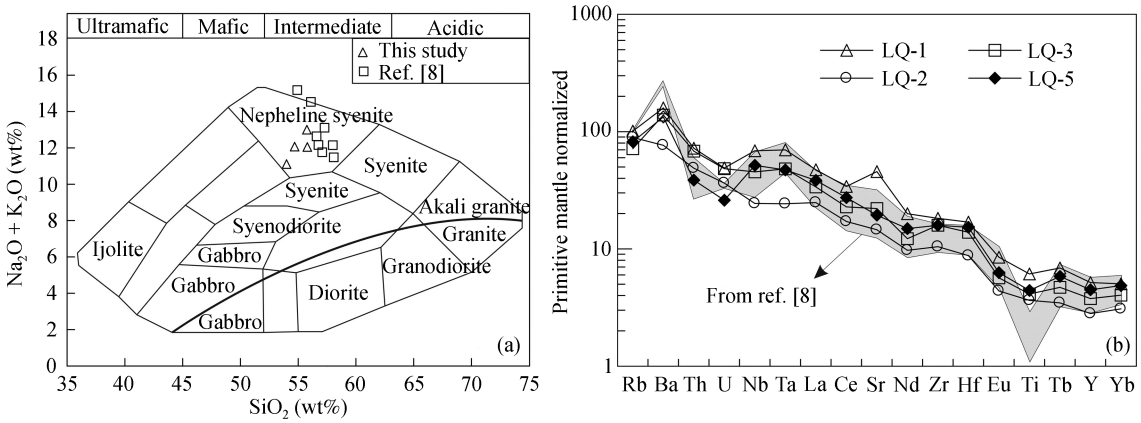

Figure 3 (a) TAS plot; (b) primitive mantle-normalized trace element abundance in the Maomaogou nepheline syenites (normalization values after ref. [21]).

Table 3 Major elements (%) and trace elements (ppm) abundance and Nd isotopic data of the Maomaogou nepheline syenites

Sample No.	LQ-1	LQ-2	LQ-3	LQ-5
SiO_2	53.99	55.75	55.79	54.69
TiO_2	0.92	0.55	0.62	0.67
Al_2O_3	19.17	20.85	20.49	19.82
$Fe_2O_3^T$	8.68	5.94	6.12	7.31
MnO	0.21	0.13	0.14	0.19
MgO	1.33	0.84	1.09	1.54
CaO	4.21	2.58	3.49	3.64
Na_2O	8.60	9.86	9.52	9.21
K_2O	2.51	3.14	2.53	2.86
P_2O_5	0.30	0.18	0.22	0.23
LOI	0.70	0.58	0.45	0.39
Total	100.00	100.00	100.00	100.00
Na_2O+K_2O	11.11	13.00	12.05	12.07
K_2O/Na_2O	0.29	0.32	0.27	0.31
Ga	23.30	22.25	22.84	23.04
Rb	60.59	53.57	42.93	49.22
Ba	1050.94	504.97	913.46	881.24
Th	5.74	3.88	5.42	3.07
U	1.00	0.74	0.98	0.53
Nb	45.25	16.04	29.87	34.00
Ta	2.59	0.90	1.78	1.75
Sr	908.69	289.58	439.48	385.72
Zr	191.28	109.64	166.89	166.95
Hf	4.78	2.48	3.91	4.32
Y	22.21	12.08	16.20	19.27
La	30.67	16.06	21.89	24.92
Ce	57.11	28.68	38.20	45.85
Nd	24.93	12.15	15.27	18.63
Sm	4.31	2.21	2.76	3.43
Eu	1.39	0.72	0.93	1.01
Gd	3.91	2.12	2.54	3.09
Tb	0.68	0.34	0.47	0.58
Yb	2.22	1.36	1.78	2.15
Nb/Ta	17.49	17.87	16.74	19.48
Eu/Eu*	1.02	1.00	1.06	0.93
$^{143}Nd/^{144}Nd$	0.512551±5	0.5124681±5	0.512492±5	0.512455±5
$\varepsilon_{Nd}(t)$[a)]	1.36	–0.44	0.06	–0.73

a) $\varepsilon_{Nd}(t)$ was calculated to be 260 Ma.

3 Genetic link between the Maomaogou intrusion and the Emeishan basalts

3.1 Temporal and spatial relationship

Intermediate/acidic alkaline intrusive rocks in the Panxi area are spatially associated with the Emeishan basalts and mafic/ultramafic intrusions. Moreover, the Emeishan basalts are intruded by mafic/ultramafic rocks, which are in turn intruded by intermediate/acidic rocks. This is further supported by chronological data. These relationships suggest that three different rocks were emplaced at the same time. The zircon U-Pb age (261.6 ± 4.4 Ma) of the Maomaogou intrusion is indistinguishable within error from those of the Xinjie ultramafic intrusion (259±3 Ma)[22], Panzhihua layer intrusion (263 ±3 Ma)[23] and Yanyuan dolerite dyke (262±3 Ma)[24]. Although no radiometric age is available for the Emeishan basalts, it can be inferred based on the occurrence of the Emeishan basalts at P_2-P_3 boundary[9] that the Emeishan volcanism was erupted during 258—260 Ma. It is therefore reasonable to propose that the Emeishan basalts, mafic/ultramafic intrusives and intermediate/acidic alkaline intrusive rocks in the Panxi area essentially have the same ages.

Lo et al.[7] reported a biotite $^{40}Ar/^{39}Ar$ age of 251—253 Ma for the Maomaogou intrusion. This age is slightly younger than the Zircon U-Pb age. This may be attributed to lower closure temperature of $^{40}Ar/^{39}Ar$ system in biotite (300—400℃)[25,26]. Liu et al. reported a zircon U-Pb age of 224±8 Ma on this intrusion. They also found two inherited ages of 622—691 Ma and 2692—2818 Ma on the basis of analyses on cores of zircons[8]. The difference between the results by Liu et al.[8]

and in this study cannot be related to sampling because it has been demonstrated previously that two independent studies were carried out on the similar rocks (Figure 3). Geochemical analyses indicate that the Maomaogou nepheline syenites are mantle-derived. Zircons in mantle-derived rocks are generally characterized by simple structure rather than complex core-rim zoning, typical of the zircons studied in this paper (Figure 2(b)). Because the primitive and depleted mantles were depleted in Zr, no zircon growth was possible during the mantle differentiation if no crustal material was involved, and zircon Hf isotope compositions in mantle-derived rocks depend on mass balance in both element concentration and isotope ratio of hafnium between mantle magma and crustal material[27]. The lowest zircon $\varepsilon_{Hf}(t)$ value in this paper is merely −1.4, suggesting no significant involvement of crustal component. On the other hand, if 2.7—2.8 Ga zircons existed, their ε_{Hf} values at 206 Ma would be lower than −40 according to the evolution trend of Hf isotopes in zircons (Figure 4). However, the observed ε_{Hf} values range from −1.4 to 4.3, again suggesting a derivation from a mantle source. On the basis of these two observations, our data seem to be superior to those of Liu et al.

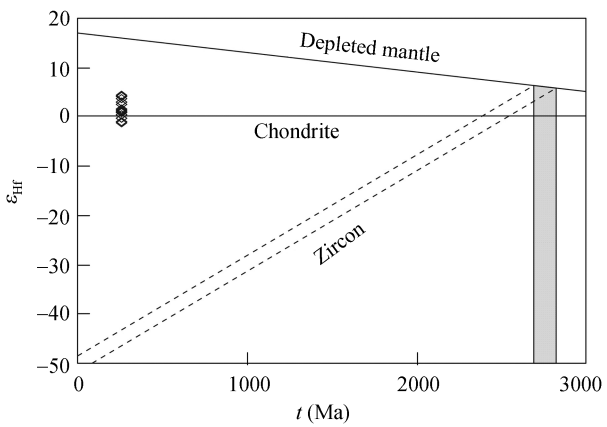

Figure 4 $\varepsilon_{Hf}(t)$ vs. age for zircons from the Maomaogou nepheline syenites. Shadow area represents ages for old cores of zircons reported by Liu et al.[8]. Dash line represents the development trend of Hf isotopes in zircon.

Geochronologic studies have been carried out on other intrusions in the Panxi area, but results are controversial[28−30]. For instance, $^{40}Ar/^{39}Ar$ dating yields a plateau age of 256 Ma on biotite separates of the Cida gabbros and a plateau age of 214—193 Ma on the whole rocks of the Jijie and Daxiangping nepheline pyroxenites. It is noted that only the age spectrum of the Cida gabbros is a planar line, and the age is consistent with Maomaogou biotite $^{40}Ar/^{39}Ar$ age[7]. By contrast, much more data scatter is noted for the other age spectrums. This suggests that the $^{40}Ar/^{39}Ar$ isotopic system in the Jijie and Daxiangping nepheline pyroxenites may have been destroyed or overprinted by later thermal events, whereas biotite $^{40}Ar/^{39}Ar$ ages for the Cida gabbros and the Maomaogou nepheline syenites reflect the cooling age of these intrusive bodies. The SHRIMP zircon U-Pb ages published by Xia et al.[30] on the Baima quartz syenite (225 Ma) and Jijie nepheline pyroxenite (204 Ma) are also misleading. It is also hard to explain the existence of zircon cores (~680 Ma and ~2000 Ma) in the Jijie ultramafic nepheline pyroxenites. More recently, Zhou et al.[1)] reported SHRIMP zircon U-Pb ages of ~260 Ma on alkaline rocks of Baima and Jijie intrusions. We believe that these ages are more meaningful.

3.2 Petrogenetic evaluation

Chen et al.[31] obtained a zircon U-Pb age of ~706 Ma for the amphibolite, and Xu et al.[32] reported an Sm-Nd isochron age of ~1140 Ma for the mafic/intermediate granulites in the Panxi area. These rocks represent the old basement of the area. $\varepsilon_{Nd}(t = 260\ Ma)$ of the amphibolite and granulite are −5.8—−2.4 and −6.7, respectively. These values are significantly different from those of the Maomaogou seynite that has $\varepsilon_{Nd}(t)$ values of −0.73 to +1.44. Therefore, the old basement cannot be the source of the Maomaogou intrusion.

Due to the similar ion radius, Nb and Ta exhibit almost identical behavior during the magmatic evolution and can be regarded as geochemical "twins"[21,33]. In most cases, Nb/Ta ratio remains almost unchanged[18,33,34]. Nb and Ta are only fractionated when Ti-rich minerals, such as rutile and titanite, are involved in magmatic system[35,36]. The Na/Ta ratio of the primitive mantle is 17.5±2.0 indistinguishable from the C1 chondrite value[18,37], whereas that of the continental crust is 11—12[34]. Therefore, Nb/Ta is the effective indicator of the crustal and mantle involvement. The Maomaogou

1) Zhou M F, et al. Geochemical constraints on a diversity of plutonic rocks of the Emeishan Large Igneous Province, SW China. 2005 Annual Symposium on Petrology and Geodynamics.

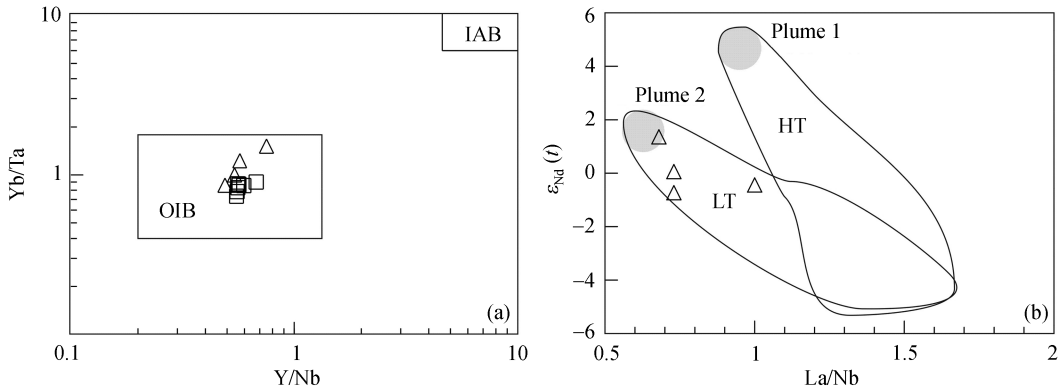

Figure 5 (a) Yb/Ta vs. Y/Nb; (b) La/Nb. Fields for OIB and IAB in (a) are after ref. [38]; Fields for LT and HT in (b) are from ref. [39].

seynite has an Nb/Ta value of 16.7—19.5 (Table 3), very similar to the mantle value. In addition, all samples are plotted in the field of oceanic island basalts (OIB) (Figure 5(a)). They also shear with the Emeishan basalts in the plot of ε_{Nd}-La/Nb (Figure 5(b)). These features suggest that the Maomaogou nepheline syenites may have been derived from a source analogue to the Emeishan basalts. Low La/Nb ratios (< 1.0) imply that they were not significantly contaminated by crust materials.

Nepheline syenites can be formed by either crystal fractionation or partial melting. If nepheline syenites are spatially associated with other mafic intrusive and silica-saturated syenites, they are generally interpreted as products of fractionation[40−42]. Given the lack of continuous rock series in the Maomaogou intrusion, the partial melting model may be more appropriate. In order to further evaluate these alternatives, we have performed a number of modeling involving major and trace element compositions.

The Maomaogou seynites exhibit no or positive Sr anomaly in the spiderdiagram (Figure 3(b)). This suggests that they unlikely represent fractionated products from the Emeishan basalts because the latter already exhibits negative Sr anomaly[39,43,44]. The Maomaogou intrusion is distributed proximally to the Longzhoushan region, where a suite of alkaline basalt-phonolite is preserved[45]. The close association leads us to select an alkaline basalt sample from Longzhoushan (LZ-22) as the hypothesized parent magma and a sample (LQ-2) from Maomaogou as daughter melt. Least squares mass balance calculations on major elements show that the transition from LZ-22 to LQ-2 involves fractionation of ~35 wt% plagioclases. Such a high proportion of plagioclase fractionation would produce a significant Sr depletion in the daughter magma (Figure 6(a)), which is not observed in the Maomaogou seynite. As a consequence, the fractionation model can be ruled out.

On the basis of experiments and geochemical elucidation, Hay et al.[46,47] proposed that Kenya rift plateau-type flood phonolites were generated by partial melting of alkali basaltic material under lower-crustal pressures. Seismic tomography reveals a high-velocity

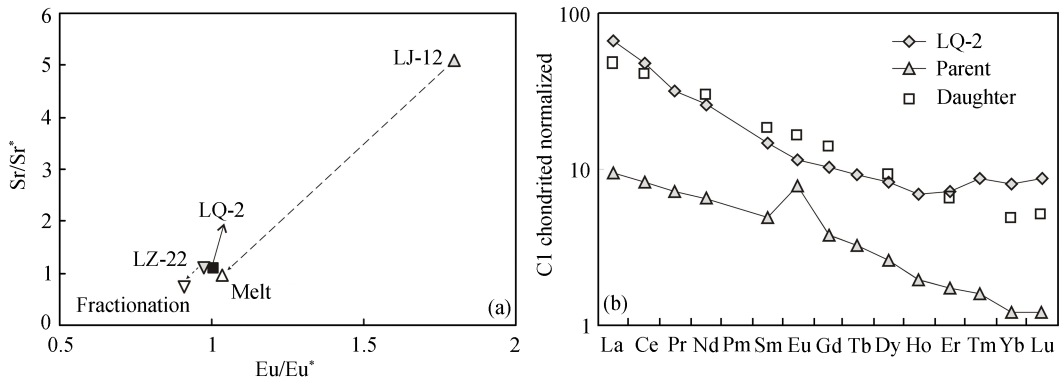

Figure 6 Comparison of modeling results with observed composition of the Maomaogou syenites. (a) Fractionation; (b) partial melting. Sr/Sr* in (a) represents the element ratio of Sr to the average of Ce and Nd, normalized by primitive mantle.

Table 4 Least squares mass balance calculations based on major elements for the Maomaogou nepheline syenites [a)]

	Parent	Daughter	Substracted phases				
	LJ-12	LQ-2	Magn	Ab	An	Cpx	Oliv
SiO_2	43.31	56.28	0.32	68.29	44	49.44	37.41
TiO_2	2.98	0.55	17.22	0.01	0	0.97	0
Al_2O_3	20.85	21.05	1.05	19.65	36.28	4.45	0
FeO^T	13.29	5.40	76.9	0.08	0.08	8.93	28.81
MnO	0.12	0.13	0.88	0	0	0.28	0
MgO	3.92	0.85	3.63	0	0	14.76	33.4
CaO	12.85	2.60	0	0.08	19.42	20.45	0.38
Na_2O	2.31	9.95	0	11.61	0.22	0.72	0
K_2O	0.37	3.17	0	0.28	0	0.01	0
Total	100.00	100.00	100	100	100	100	100

Daughter	Σr^2	Percentage (%)	Percentage of substracted phases (%)				
			Magn	Ab	An	Cpx	Oliv
LQ-2	0.18	5.22	14.26	15.32	43.09	21.62	0.48

a) Magn, magnetite; Ab, albite; An, anorthite; Cpx, clinopyroxene; Oliv, olivine.

lower crust (V_p = 7.1—7.8 km/s) in the Panxi area[48], which has been attributed to the underplating of plume-derived basaltic melts in the crust-mantle boundary[9]. The pressure condition and basaltic composition of the lower crust in the Panxi area are very similar to those of partial melting model put forward by Hay et al.[46,47]. On the other hand, positive Sr anomaly of the Maomaogou intrusion implies that its source may contain plagioclase-rich cumulates. This is further confirmed by petrologic modeling which suggests that the high-velocity lower crust is composed of gabbroic cumulates[49].

To test the partial melting model, mass balance calculation (see ref. [50] for detailed calculation procedures) has been performed by selecting a cumulate gabbro sampled from the Panzhihua layered intrusion as the source rock, and the sample LQ-2 with the lowest REE content in nepheline syenites as partial melting product. The result shows that nepheline syenites can be formed by ~5% partial melting of gabbroic cumulates (Table 4). The proportions of subtracted phases calculated in terms of major element modeling are used to model the REE variation during partial melting. The results show that the modeled REE composition of partial melts is very similar to that of LQ-2 (Figure 6(b)). All these suggest that partial melting of gabbroic cumulates is a feasible model to generate the Maomaogou nepheline syenites. On the basis of their element and isotope features, the gabbroic cumulates have geochemical affinity to the juvenile crust of mafic composition and thus probably formed by underplating of basaltic magma. Therefore, further studies are necessary in order to make distinction between the following three possible origins: (1) partial melting of the Emeishan mantle plume head in the latest Paleozoic[9], (2) mafic magmatism in association with subduction of oceanic crust during assembly of the supercontinent Rodinia in South China at 1.0—0.9 Ga[51], (3) rift magmatism in synchronism with the Rodinia breakup in South China at about 750 Ma[27].

In summary, temporal coincidence, spatial relationship and petrogenetic link between the Maomaogou syenite and the Emeishan basalts strongly suggest that the alkaline intrusive rock is an integral part of the Emeishan LIP. The close association of basalts, mafic/ultramafic and intermediate/acidic alkaline intrusive rocks in the Panxi area highlights one of major features of this large igneous province.

The authors would like to thank the two anonymous reviewers for their constructive comments. Discussion with Dr. Yang Jinhui was very helpful.

1 Mathoney J J, Coffin M. Large igneous provinces: Continental, oceanic and planetary flood volcanism. Washington D C: AGU Geophysical Monography, 1997. 1—438

2 Courtillot V, Jaupart C, Manighetti I, et al. On causal links between flood basalts and continental breakup. Earth Planet Sci Lett, 1999, 166: 177—195

3 Wignall P B. Large igneous provinces and mass extinctions. Earth Sci Rev, 2001, 53: 1—33

4 Ali J R, Lo C H, Thompson G M, et al. Emeishan Basalt Ar-Ar overprint ages define several tectonic events that affected the western

Yangtze Platform in the Mesozoic and Cenozoic. J Asian Earth Sci, 2004, 23: 163－178
5 Boven A, Pasteels P, Punzalan L E, et al. $^{40}Ar/^{39}Ar$ geochronological constraints on the age and evolution of the Permo-Triassic Emeishan Volcanic Province, Southwest China. J Asian Earth Sci, 2002, 20: 157－175
6 Zhang Y X, Luo Y N, Yang C X. Panxi Rift (in Chinese). Beijing: Geological Publishing House, 1988. 1－325
7 Lo C H, Chung S L, Lee T Y, et al. Age of the Emeishan flood magmatism and relations to Permian-Triassic boundary events. Earth Planet Sci Lett, 2002, 198: 449－458
8 Liu H Y, Xia B, Zhang Y Q. Zircon SHRIMP dating of sodium alkaline rocks from Maomaogou area of Huili County in Panxi, SW China and its geological implications. Chin Sci Bull, 2004, 49(16): 1750－1757
9 Xu Y G, He B, Chung S L, et al. Geologic, geochemical, and geophysical consequences of plume involvement in the Emeishan flood-basalt province. Geology, 2004, 32: 917－920
10 He B, Xu Y G, Chung S L, et al. Sedimentary evidence for a rapid, kilometer-scale crustal doming prior to the eruption of the Emeishan flood basalts. Earth Planet Sci Lett, 2003, 213: 391－405
11 Compston W, Williams I S, Meyer C. U-Pb geochronology of zircons from lunar breccia 73217 using a sensitive high mass-resolution ion microprobe. J Geophys Res, 1984, 89: B525－534
12 Williams I S. Some observations on the use of zircon U-Pb geochronology in the study of granitic-rocks. Trans R Soc Edinburgh-Earth Sci, 1992, 83: 447－458
13 Vavra G, Gebauer D, Schmid R, et al. Multiple zircon growth and recrystallization during polyphase Late Carboniferous to Triassic metamorphism in granulites of the Ivrea Zone (Southern Alps): An ion microprobe (SHRIMP) study. Contri Mineral Petrol, 1996, 122: 337－358
14 Vavra G, Schmid R, Gebauer D. Internal morphology, habit and U-Th-Pb microanalysis of amphibolite-to-granulite facies zircons: geochronology of the Ivrea Zone (Southern Alps). Contri Mineral Petrol, 1999, 134: 380－404
15 Wu Y B, Zheng Y F. Genesis of zircon and its constraints on interpretation of U-Pb age. Chin Sci Bull, 2004, 49(15): 1554－1569
16 Rubatto D, Gebauer D. Use of cathodoluminescence for U-Pb Zircon Dating by IOM Microprobe: Some Examples from the Western Alps. Berlin-Heidelberg: Springer-Verlag, 2000. 373－400
17 Moeller A, O'Brien P J, Kennedy A, et al. Linking growth episodes of zircon and metamorphic textures to zircon chemistry; an example from the ultrahigh-temperature granulites of Rogaland, SW Norway. In: Vance D, Muller W, Villa I M, eds. Geochronology: Linking the Isotopic Record with Petrology and Textures. Bath: Geological Soc Publishing House, 2003. 65－81
18 Xu P, Wu F Y, Xie L W, et al. Hf isotopic compositions of the standard zircons for U-Pb dating. Chin Sci Bull, 2004, 49(15): 1642－1648
19 Goolaerts A, Mattielli N, de Jong J, et al. Hf and Lu isotopic reference values for the zircon standard 91500 by MC-ICP-MS. Chem Geol, 2004, 206: 1－9
20 Woodhead J, Hergt J, Shelley M, et al. Zircon Hf-isotope analysis with an excimer laser, depth profiling, ablation of complex geometries, and concomitant age estimation. Chem Geol, 2004, 209: 121－135
21 Sun S S, McDonough W F. Chemical and isotopic systematics of oceanic basalts: implications for mantle composition and processes. Geological Society Special Publications, 1989. 313－345
22 Zhou M F, Malpas J, Song X Y, et al. A temporal link between the Emeishan large igneous province (SW China) and the end-Guadalupian mass extinction. Earth Planet Sci Lett, 2002, 196: 113－122
23 Zhou M F, Robinson P T, Lesher C M, et al. Geochemistry, petrogenesis and metallogenesis of the Panzhihua gabbroic layered intrusion and associated Fe-Ti-V oxide deposits, Sichuan Province, SW China. J Petrol, 2005, 46: 2253－2280
24 Guo F, Fan W M, Wang Y J, et al. When did the emeishan mantle plume activity start? Geochronological and geochemical evidence from ultramafic-mafic dikes in southwestern China. Internat Geol Rev, 2004, 46: 226－234
25 Harrison T M, Duncan I, McDougall I. Diffusion of ^{40}Ar in biotite; temperature, pressure and compositional effects. Geochim Cosm Acta, 1985, 49: 2461－2468
26 Berger G W, York D. Geothermometry from $^{40}Ar/^{39}Ar$ dating experiments. Geochim Cosm Acta, 1981, 45: 795－811
27 Zheng Y F, Zhao Z F, Wu Y B, et al. Zircon U-Pb age, Hf and O isotope constraints on protolith origin of ultrahigh-pressure eclogite and gneiss in the Dabie orogen. Chem Geol, 2006, 231: 135－158
28 Liu H Y, Xia B, Liang H Y, et al. Geochronology of layered intrusions in Cida and Taihe Districts, Panxi Area, Sichuan Province. Geol J China Universities (in Chinese), 2004, 10: 179－185
29 Liu H Y, Xia B, Zhang Y Q. ^{40}Ar-^{39}Ar ages of the ultrabasic alklic rock and layered gabbro in Panzhihua-Xichang rift zone: examples from the Jijie, Daxiangping and Taihe pluton. Geol Rev (in Chinese), 2004, 50: 175－179
30 Xia B, Liu H Y, Zhang Y Q. SHRIMP dating of agpaitic alkalic rocks in Panxi rift zone and its geological implications – examples for Hongge, Baima and Jijie rock bodies. Geotectonica et Metallogenia (in Chinese), 2004, 28: 149－154
31 Chen Y L, Luo Z H, Zhao J X, et al. Petrogenesis and dating of the Kangding complex, Sichuan Province. Sci China Ser D-Earth Sci, 2005, 48(5): 622－634
32 Xu S J, Liu W Z, Wang R C, et al. The history of crustal uplift and metamorphic evolution of Panzhihua-Xichang micro-palaeoland, SW China: $^{40}Ar/^{39}Ar$ and FT ages of granulites. Sci China Ser D-Earth Sci, 2004, 47(8): 689－703

33 Jochum K P, Seufert H M, Spettel B, et al. The solar-system abundances of Nb, Ta, and Y, and the relative abundances of refractory lithophile elements in differentiated planetary bodies. Geochim Cosmochim Acta, 1986, 50: 1173－1183
34 Green T H. Significance of Nb/Ta as an Indicator of Geochemical Processes in the Crust-Mantle System. Chem Geol, 1995, 120: 347－359
35 Green T H, Pearson N J. An experimental study of Nb and Ta partitioning between Ti-rich minerals and silicate liquids at high pressure and temperature. Geochim Cosmochim Acta, 1987, 51: 55－62
36 Niu Y L, Batiza R. Trace element evidence from seamounts for recycled oceanic crust in the Eastern Pacific mantle. Earth Planet Sci Lett, 1997, 148: 471－483
37 Weyer S, Munker C, Rehkamper M, et al. Determination of ultra-low Nb, Ta. Zr and Hf concentrations and the chondritic Zr/Hf and Nb/Ta ratios by isotope dilution analyses with multiple collector ICP-MS. Chem Geol, 2002, 187: 295－313
38 Eby G N. Chemical subdivision of the A-type granitoids; petrogenetic and tectonic implications. Geology, 1992, 20: 641－644
39 Xu Y G, Chung S L, Jahn B M, et al. Petrologic and geochemical constraints on the petrogenesis of Permian-Triassic Emeishan flood basalts in southwestern China. Lithos, 2001, 58: 145－168
40 Eby G N, Woolley A R, Din V, et al. Geochemistry and petrogenesis of nepheline syenites: Kasungu-Chipala, Ilomba, and Ulindi nepheline syenite intrusions, North Nyasa Alkaline Province, Malawi. J Petrol, 1998, 39: 1405－1424
41 Worley B A, Cooper A F, Hall C E. Petrogenesis of carbonate-bearing nepheline syenites and carbonatites from Southern Victoria Land, Antarctica - Origin of carbon and the effects of calcite-graphite equilibrium. Lithos, 1995, 35: 183－199
42 Yang J H, Chung S L, Wilde S A, et al. Petrogenesis of post-orogenic syenites in the Sulu Orogenic Belt, East China: geochronological, geochemical and Nd-Sr isotopic evidence. Chem Geol, 2005, 214: 99－125
43 Xiao L, Xu Y G, Chung S L, et al. Chemostratigraphic correlation of upper permian lavas from Yunnan province, China: Extent of the Emeishan large igneous province. Internat Geol Rev, 2003, 45: 753－766
44 Xiao L, Xu Y G, Mei H J, et al. Distinct mantle sources of low-Ti and high-Ti basalts from the western Emeishan large igneous province, SW China: implications for plume-lithosphere interaction. Earth Planet Sci Lett, 2004, 228: 525－546
45 Mei H J, Xu Y G, Xu J F, et al. Late Permian basalt-phonolite suite from Longzhoushan in the Panxi rift zone. Acta Geol Sin (in Chinese), 2003, 77: 341－358
46 Hay D E, Wendlandt R F. The origin of Kenya Rift Plateau-Type flood phonolites——Results of high-pressure high-temperature experiments in the systems phonolite-H_2O and phonolite-H_2O-CO_2. J Geophys Res-Solid Earth, 1995, 100: 401－410
47 Hay D E, Wendlandt R F, Wendlandt E D. The origin of Kenya Rift Plateau-Type Flood phonolites - evidence from geochemical studies for fusion of lower crust modified by alkali basaltic magmatism. J Geophys Res-Solid Earth, 1995, 100: 411－422
48 Liu J H, Liu F T, He J K, et al. Study of seismic tomography in Panxi paleorift area of southwestern China——Structural features of crust and mantle and their evolution. Sci China Ser D-Earth Sci, 2001, 44(3): 277－289
49 Zhu D, Luo T Y, Gao Z M, et al. Differentiation of the Emeishan flood basalts at the base and throughout the crust of southwest China. Interna Geol Rev, 2003, 45: 471－477
50 Wright T L, Doherty P C. A linear programming and least squares computer method for solving petrologic mixing problems. GSA Bull, 1970, 81: 1995－2007
51 Wu R X, Zheng Y F, Wu Y B, et al. Reworking of juvenile crust: Element and isotope evidence from Neoproterozoic granodiorite in South China. Precambrian Res, 2006, 146: 179－212